**Supporting Information**

Fabrication and notable optical nonlinearities of ultrathin composite films derived from the water-soluble Keggin-type polyoxometalates and water-insoluble phthalocyanine
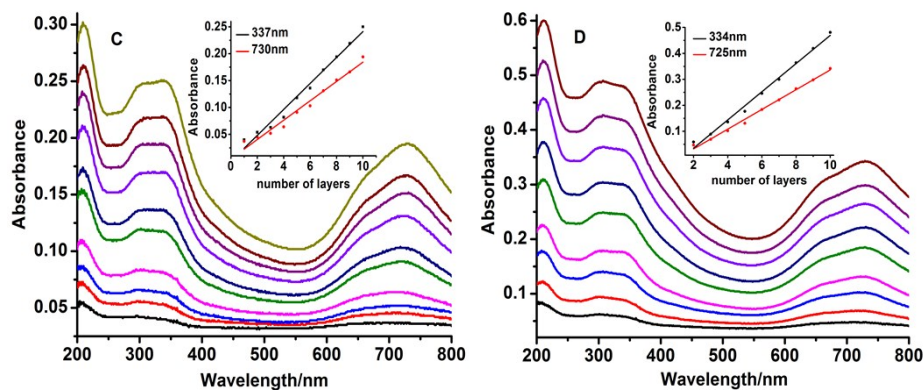
Farooq K. Shehzad,[†] Ningning Qu,[†] Yunshan Zhou,[*] Lijuan Zhang,[*] Huanyao Ji, Zonghai Shi

Jiaqi Li and Sadaf Ul Hassan

State Key Laboratory of Chemical Resource Engineering, Institute of Science, Beijing

University of Chemical Technology, Beijing 100029, P. R. China
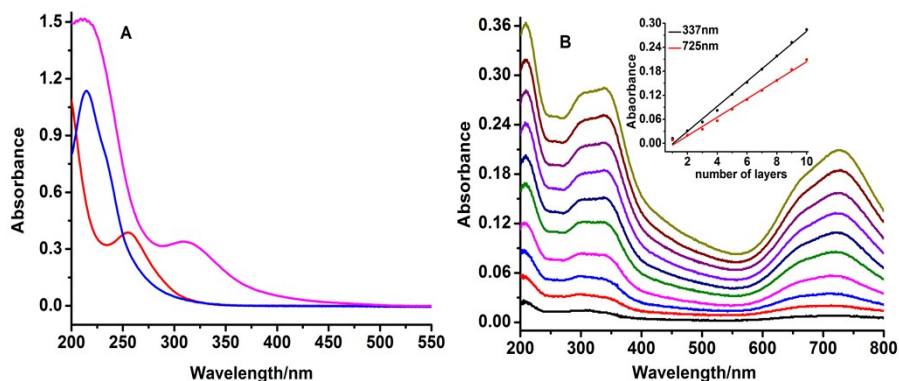
Figure S1 UV-vis spectra of PW (red); PMo (blue); PMoV (pink) in water (A) and composite films (PAH/PSS/PAH)(POM/CuPTAs)$_n$ (B - D):(PW/CuPTAs)$_n$ (B), (PMo/CuPTAs)$_n$, (C) and (PMoV/CuPTAs)$_n$ (D). Lines from bottom to top for each figure correspond to n = 1 ~ 10, respectively. Inset: the plots of absorbance values for composite films at corresponding wavelength as a function of n.

It is found that absorbance intensity at 306 nm has an increase at both SiW and CuTAPc adsorption steps, while absorbance intensity at 728 nm has an increase only at the CuTAPc adsorption steps because there is no absorbance for SiW. Thus, the incremental increase is smaller at 728 nm as compared to that at 306 nm. The absorbance at 336, 728 nm increases gradually with the number of SiW/ CuTAPc layers, indicating SiW and CuTAPc are smoothly and constantly integrated in the multilayer.

The UV-vis absorption spectra of Keggin-type POMs in aqueous solution are shown in Fig. S1. The maximum absorption band appearing at 255 nm for PW, 214 nm for PMo and 213 nm for PMoV can be assigned to bridge oxygen to tungsten/molybdenum charge transfer transition. The absorbance at 312 nm for PMoV is the typical absorption of polyoxometalates containing vanadium (H. So and. M. T Pope, *Inorg. Chem.* **1972,** *11*, 1441-1443; M. T. Pope,. *Heteropoly and isopoly oxometalates;* Springer Verlag,1983.).
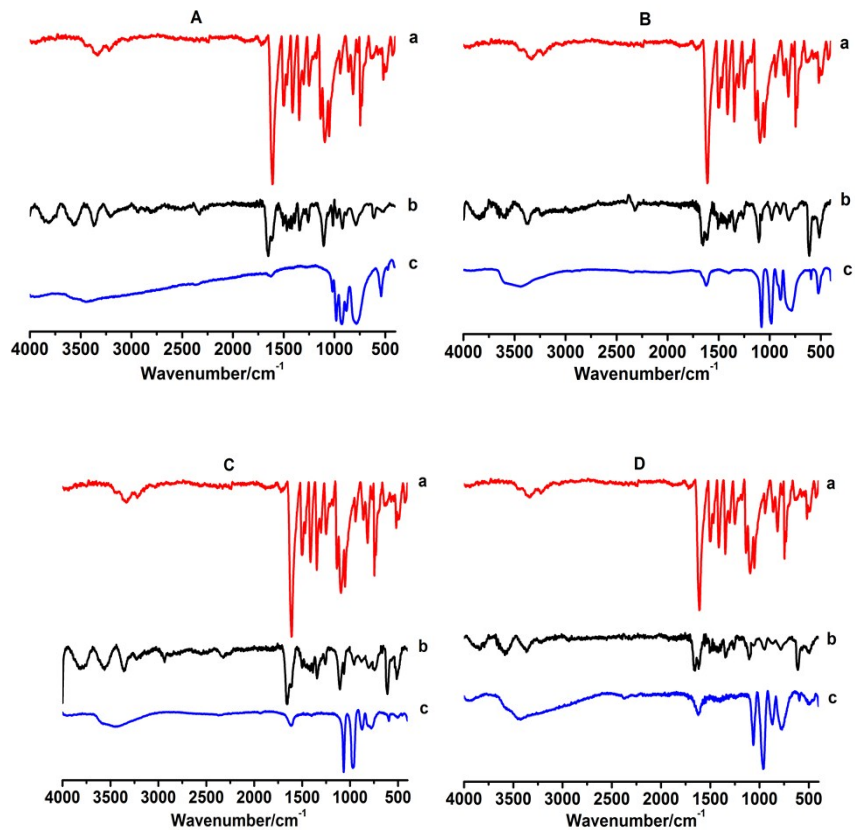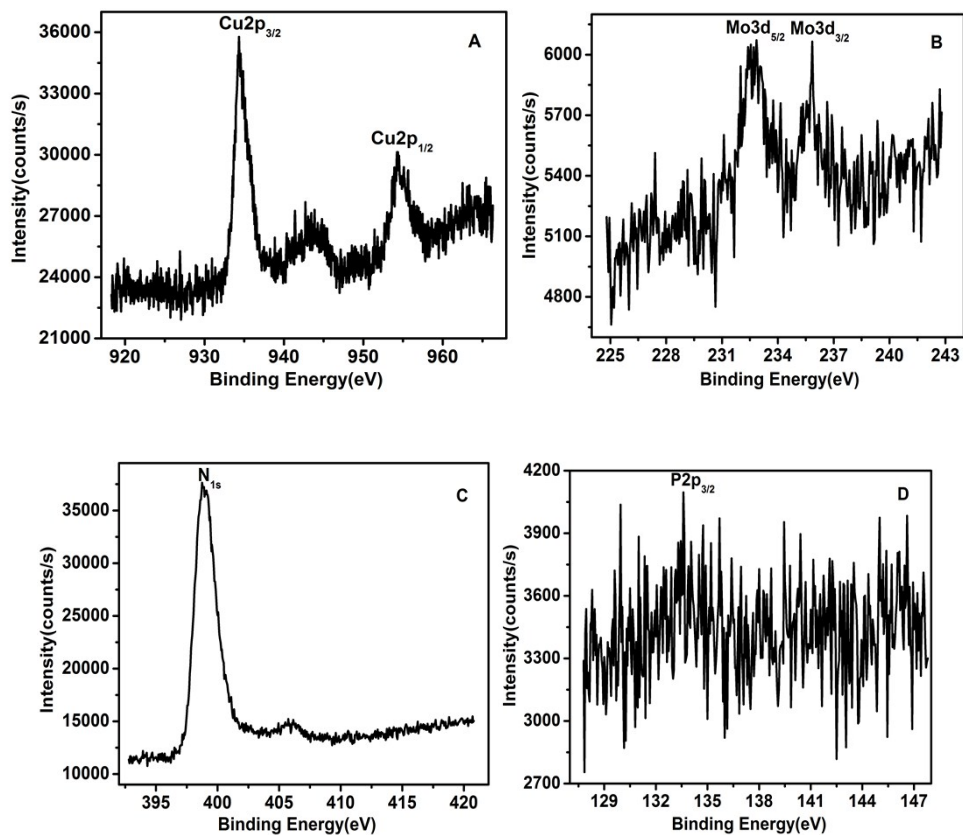
Figure S2 FTIR spectra of the composite films (PAH/PSS/PAH)(POM/CuPTAs)$_{60}$ where in POM = SiW (A), PW (B), PMo (C) and PMoV (D). The curves a, b, c correspond to the FTIR of CuPTAs, (POM/CuPTAs)$_{60}$, and POMs, respectively, in (A), (B), (C) and (D).
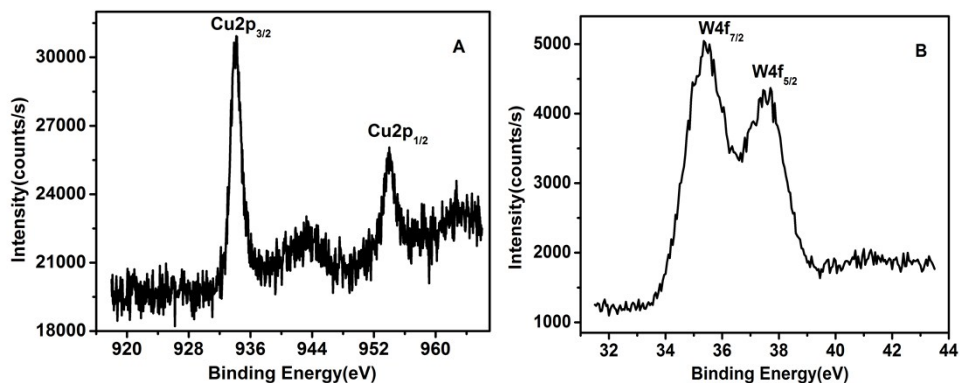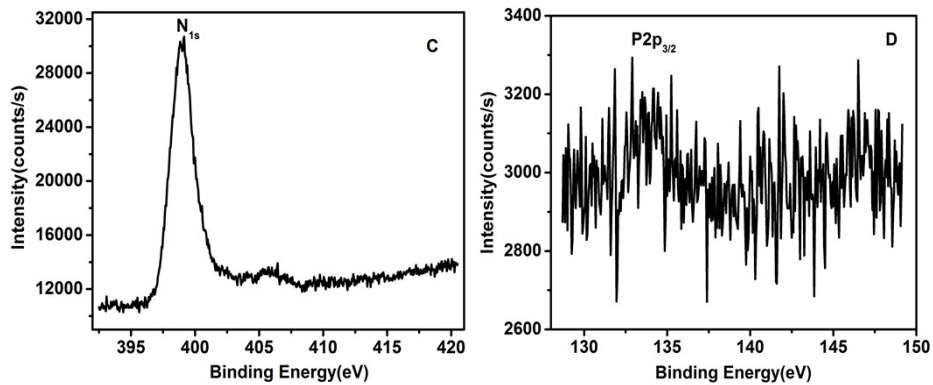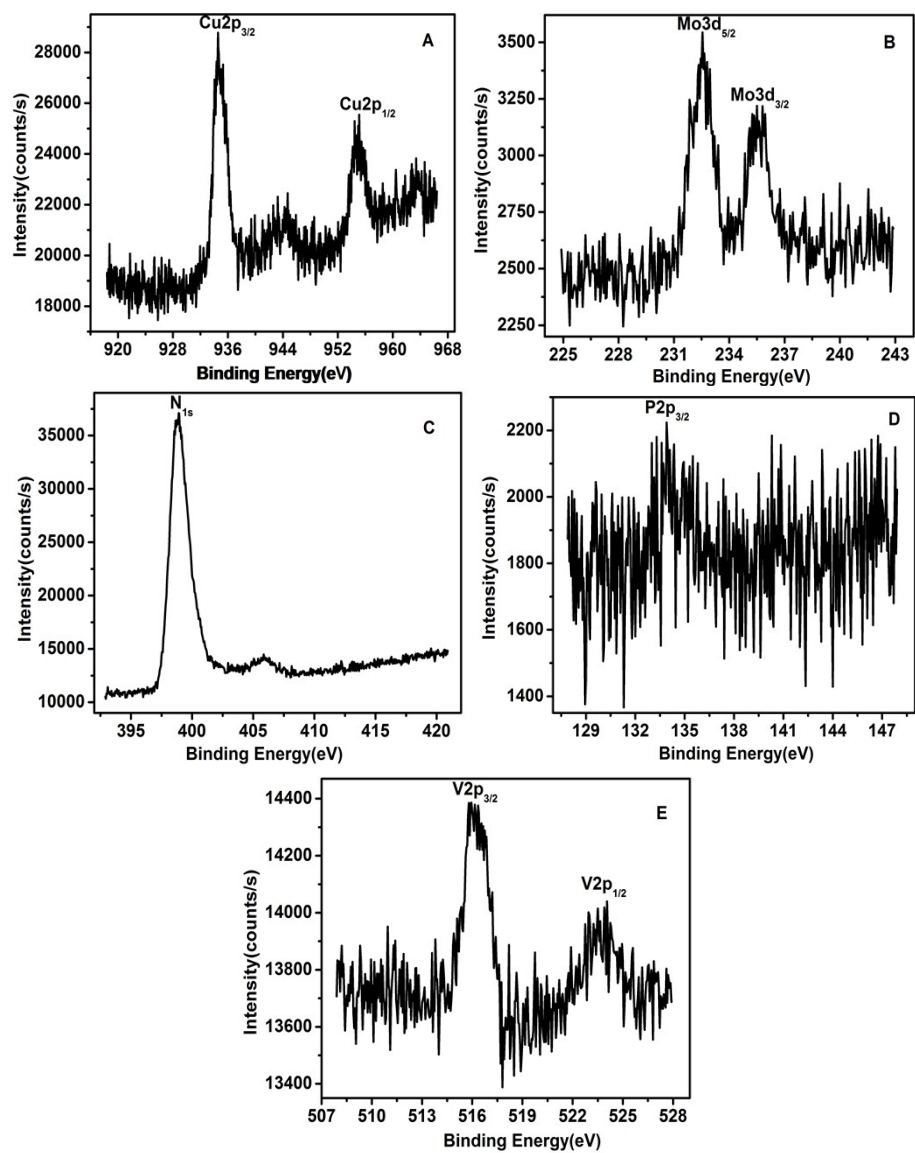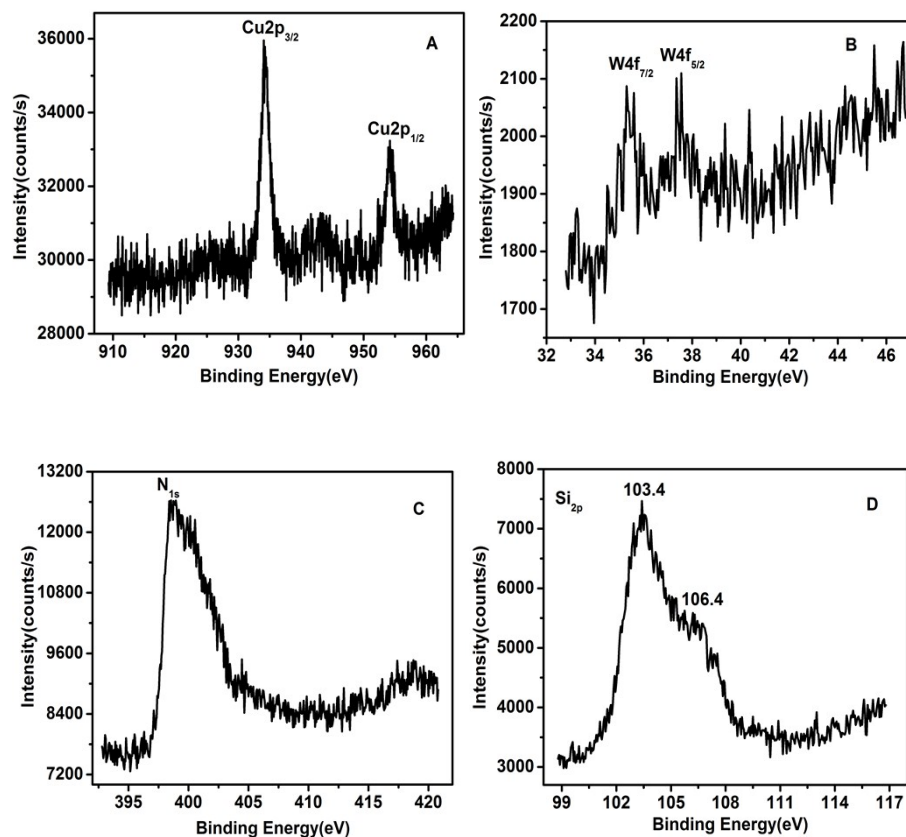
Figure S3 XPS spectra of the composite film (PAH/PSS/PAH)(PW/CuPTAs)$_5$. A: Cu$_{2p}$; B: W$_{4f}$; C: N$_{1s}$; D: P$_{2p}$

Figure S4 XPS spectra of the composite film (PAH/PSS/PAH)(PMo/CuPTAs)$_5$. A: Cu$_{2p}$; B: Mo$_{3d}$; C: N$_{1s}$; D: P$_{2p}$.

Figure S5 XPS spectra of the composite film (PAH/PSS/PAH)(PMoV/CuPTAs)$_5$.A: Cu$_{2p}$; B: Mo$_{3d}$; C: N$_{1s}$; D: P$_{2p}$; E: V$_{2p}$.

Figure S6 XPS spectra of the composite film (PAH/PSS/PAH)(SiW/CuPTAs)$_5$. A: Cu$_{2p}$; B: W$_{4f}$;
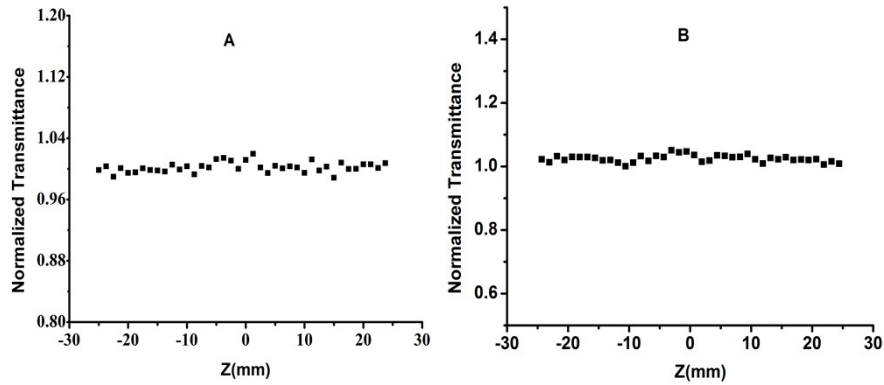
C: N$_{1s}$; D：Si$_{2p}$.
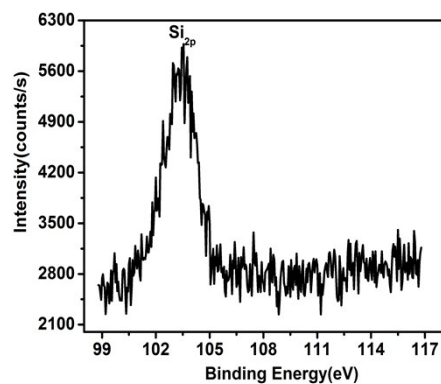
Figure S7 XPS spectrum of Si in glass substrate

Table S1 XPS data of the POMs/CuTAPc films

Films	Cu $2p_{1/2}$	Cu $2p_{3/2}$	N $1s$	P(Si)2p	W $4f_{7/2}$	W $4f_{5/2}$	Mo $3d_{5/2}$	Mo $3d_{3/2}$	V $2p_{1/2}$	V $2p_{3/2}$
(SiW/CuTAPc)$_5$	954.3	934.1	398.6	106.4	35.3	37.5	—		—	
(PW/CuTAPc)$_5$	954.0	934.2	399.0	133.6	35.4	37.5	—		—	
(PMo/CuTAPc)$_5$	954.4	934.5	398.8	133.6	—		232.8	235.8	—	
(PMoV/CuTAPc)$_5$	954.5	934.4	398.9	134.1	—		232.6	235.5	515.9	523.5

Figure S8 Z-scan curves of precursor films (PAH/PSS)$_3$ modified quartz substrate under open-aperture configuration (A) and closed-aperture configuration (B).
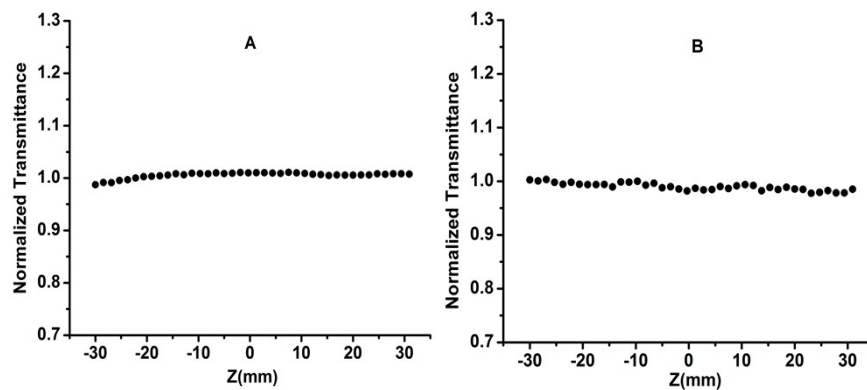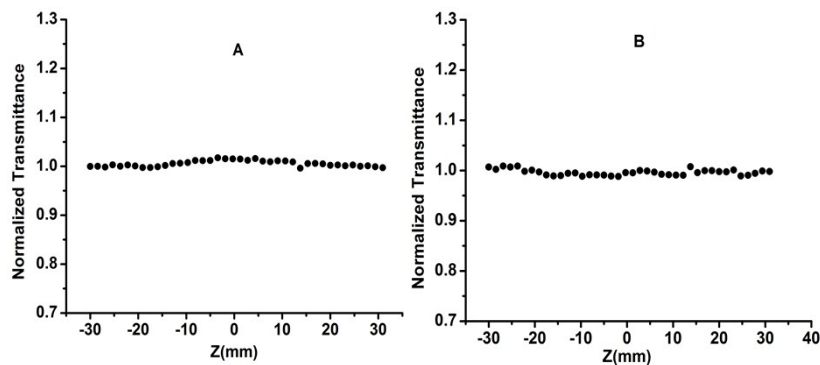
Figure S9 Z-scan curves of SiW in H_2O (10^{-3} M), (A) the open-aperture configuration (B) the closed-aperture configuration.
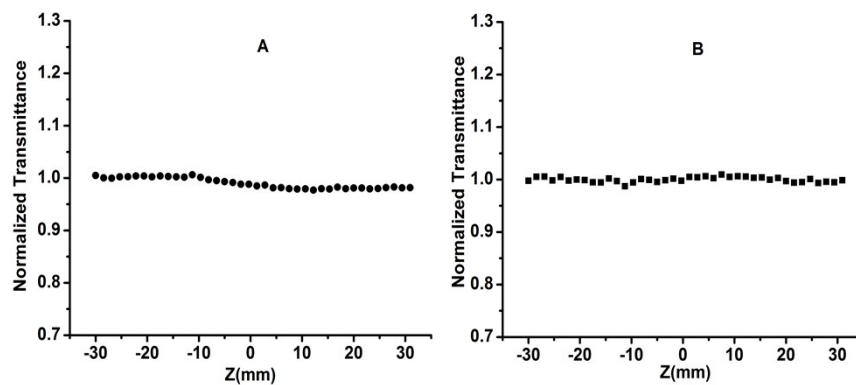
Figure S10 Z-scan curves of PW in H_2O (10^{-3} M), (A) the open-aperture configuration (B) the closed-aperture configuration.

Figure S11 Z-scan curves of PMo in H_2O (10^{-3} M), (A) the open-aperture configuration (B) the closed-aperture configuration.
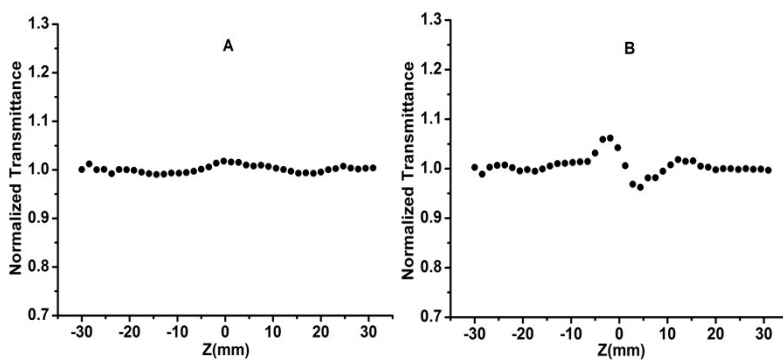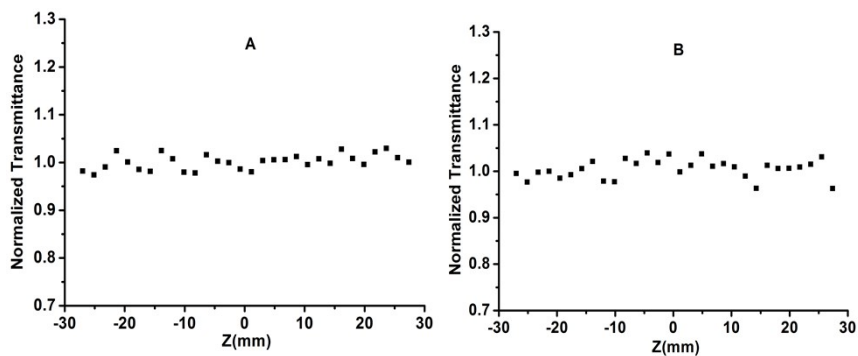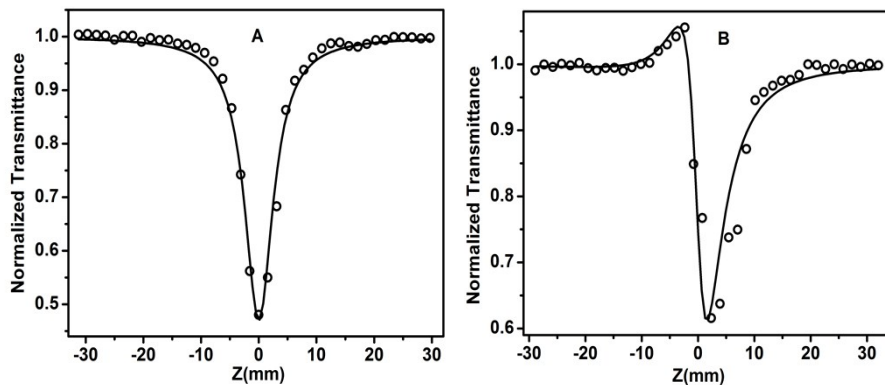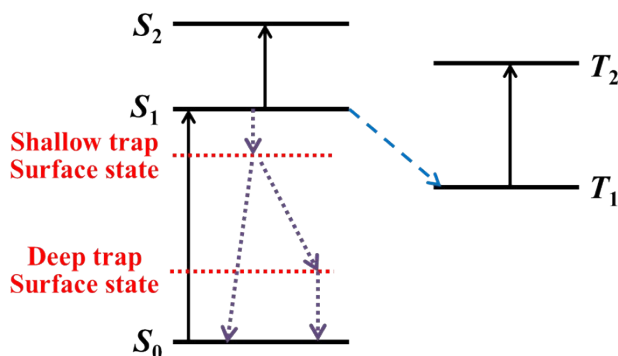

Figure S12 Z-scan curves of PMoV in H_2O (10^{-3} M), (A) the open-aperture configuration (B) the closed-aperture configuration.

Figure S13 Z-scan curves of DMF solvent, (A) the open-aperture configuration (B) the closed-aperture configuration.

Figure S14 Z-scan curves of CuPTAs in DMF (10^{-4} M), (A) the open-aperture configuration (B) the closed-aperture configuration.

Figure S15 Schematic diagram of surface state trapping formed in film $(PSS/CuTAPc)_n$

The calculation formulas of third-order nonlinear optical parameters

The following formulas are used to calculate the third-order nonlinear refractive index n_2 (esu), the nonlinear absorption coefficient β (esu) and the third-order optical nonlinear susceptibility $\chi^{(3)}$ (esu) (Sheik-Bahae, M. Said, A. A. Van and E. W. Stryland, *Opt. lett.* **1989,** *14*, 955-957.):

$$\Delta T_{P-V} = 0.406(1-S)^{0.25}|\Delta\phi_0| \quad (1)$$

$$\Delta\phi_0 = kL_{eff}\gamma I_0 \quad (2)$$

$$L_{eff} = (1 - e^{-\alpha_0 L}) / \alpha_0 \quad (3)$$

$$n_2(esu) = \frac{cn_0}{40\pi} \gamma (m^2/W) \quad (4)$$

where, ΔT_{P-V} is the normalized peak-valley difference, $\Delta\varphi_0$ is the phase shift of the beam at the focus, $K = 2\pi/\lambda$ is the wave vector, I_0 (unit: W/m^2) is the intensity of the light at focus, L_{eff} is the effective length of the sample defined in terms of the linear-absorption coefficient α_0 and the true optical path length through the sample, n_0 is the linear refractive index, and γ is optical Kerr constant. The conversion can be done between n_2 (esu) and γ (m^2/W) by eq (4).

When the sample is measured under open aperture, the normalized transmittance T $(z, s = 1)$ can be expressed as

$$T(z, s = 1) = \sum_{m=0}^{\infty} \frac{[-q_0(z)]^m}{(m+1)^{3/2}} \quad (5)$$

Where

$$q_0(z) = \frac{\beta I_0 L_{eff}}{(1 + z^2/z_0^2)},$$

β is nonlinear absorption coefficient.

From eq (5) we can get β. From eq (6), we can get the third-order optical nonlinear susceptibility $\chi^{(3)}$.

$$\chi^{(3)} = \sqrt{(\frac{cn_0}{160\pi^2}\gamma)^2 + (\frac{c\beta n_0^3 \lambda}{64\pi^3})^2} \quad (6)$$